

Depositing light in a photonic stop gap by use of Kerr nonlinear microresonators

Philip Chak and J. E. Sipe

Department of Physics, University of Toronto, Toronto, Ontario M5S 1A7, Canada

Suresh Pereira

Institut für Theorie der Kondensierten Materie, Universität Karlsruhe, 76128 Karlsruhe, Germany

Received June 18, 2003

We show theoretically that it is possible to trap light in a microresonator structure by use of four-wave mixing. The efficiency of the parametric process is substantially increased by the high group delay of light inside the structure. The energy that is trapped has a half-life of approximately 500 ps in the presence of both linear and nonlinear loss in the channel waveguides and resonators. We also demonstrate that the energy can be extracted from the cavity with a similar process. © 2003 Optical Society of America

OCIS codes: 190.4410, 230.7380, 230.5750, 140.7010.

Both Kerr nonlinear parametric processes¹ and self-phase modulation²⁻⁵ can be substantially enhanced in a system of microring resonators coupled to channel waveguides. In this Letter we combine these observations and present a scheme for trapping and releasing light from a photonic stop gap. We consider the model system shown in Fig. 1(a), which consists of two channel waveguides and four microresonators, all of which are Kerr nonlinear. The two outer resonators (shaded), with resonant frequency ω_o , act as frequency-selective mirrors, because light traveling in the forward (backward) direction in the lower channel is coupled via the outer resonators to light traveling in the backward (forward) direction in the upper channel. If the frequency of the light is an integer multiple of ω_o , then the effect of this coupling is enhanced, and the structure is 100% reflecting. The two enhancement resonators (unshaded) couple only to the lower waveguide; their effect is to enhance any Kerr nonlinear processes for light with a frequency that is an integer multiple of ω_e .

The structure traps light as follows. A strong pump and a weak idler pulse with carrier frequencies ω_p and ω_i , respectively [dotted lines in Fig. 1(b)], are injected into the system along the lower channel. Because ω_p and ω_i are not integer multiples of ω_o , neither pulse is reflected at the outer resonators. They are, however, integer multiples of ω_e , so that their parametric upconversion is enhanced, and there is much larger buildup of signal light at $\omega_s = 2\omega_p - \omega_i$ than would be expected given the $\approx 100\text{-}\mu\text{m}$ length of the structure. The frequency of the signal light is an integer multiple of both ω_o and ω_e [Fig. 1(b)]; consequently the signal light generated inside the enhancement resonators is trapped within the structure by the outer resonators. To extract the trapped light, we use a flush pulse with frequency $\omega_f = \omega_p$ to shift the frequency of the signal light with cross-phase modulation, so that it can escape from the system. Although similar to a scheme recently proposed for fiber Bragg gratings,⁶ our scheme has the advantages of a flushing technique and much

smaller dimensions. Although not of immediate practical engineering interest, our scheme illustrates the fascinating low-intensity nonlinear effects these semiconductor microstructures can exhibit.

We define the envelope functions $A_p(z, t)$, $A_i(z, t)$, and $A_s(z, t)$, carried at frequencies ω_p , ω_i , and ω_s , respectively, where $|A_{p/i/s}|^2$ gives the intensity in the field. We assume that coupling between the channel waveguides and the microresonators occurs only at the discrete points indicated by the large dots in Fig. 1(a); we call these coupling points. At the coupling points we define the self-coupling (σ) and cross-coupling (κ) coefficients and assume²

$$\begin{pmatrix} E_3 \\ E_2 \end{pmatrix} = \begin{bmatrix} \sigma & i\kappa \\ i\kappa & \sigma \end{bmatrix} \begin{pmatrix} E_4 \\ E_1 \end{pmatrix},$$

where a typical set of fields, E_m , which can represent the pump, idler, or signal field, is shown in Fig. 1(a). To conserve energy, the coupling coefficients must satisfy $|\sigma|^2 + |\kappa|^2 = 1$ and $\sigma^* \kappa = \sigma \kappa^*$. The use of such

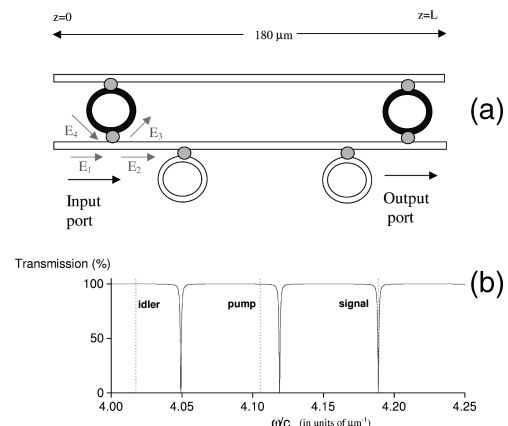


Fig. 1. (a) Schematic of the system. All pulses are injected along the bottom channel. (b) Transmission spectrum (solid curve) of the structure, the dips correspond to resonances of the outer resonators. The dotted lines correspond to resonances of the inner resonators.

phenomenological coupling coefficients has been shown to be valid for microresonator structures in the linear regimes.^{2,7,8} A rough estimate (following Ref. 9) of the nonlinear change in the evanescent fields responsible for coupling leads to such a small effect that we neglect it here, which is in line with other studies.^{1,2} Therefore we assume that there is no nonlinearity in a small region around the coupling points, which simplifies the numerics without affecting the physics. Away from the coupling points we model the propagation of light with a set of coupled nonlinear equations. We introduce a generalized length variable ζ , with $\zeta = \pm z$ in the channel guides, and $\zeta = R_{e/o}\theta$ in the resonators, where $R_{e/o}$ is the radius of the enhancement/outer resonator. With the strong pump approximation, $|A_p|^2 \gg |A_i|^2, |A_s|^2$, and with n_2 being the Kerr nonlinear coefficient and $\alpha_1, \alpha_2, \alpha_3$ being the linear, two-, and three-photon absorption (2PA and 3PA) loss coefficients, respectively, we find

$$\left(\frac{\partial}{\partial \zeta} + \frac{1}{v_g} \frac{\partial}{\partial t}\right) A_q = i\gamma_q K_q - \frac{1}{2} L_q A_q, \quad (1)$$

where q is one of (p, i, s) and $\gamma_q = \omega_q n_2 / c$. Here $K_p = |A_p|^2 A_p + 2A_s A_i A_p^*$ and $K_{i,s} = |A_{i,s}|^2 A_{i,s} + 2A_p^2 A_{s,i}^*$ account for Kerr nonlinear effects, and $L_p = \alpha_1 + \alpha_2 |A_p|^2 + \alpha_3 |A_p|^4$ and $L_{i,s} = \alpha_1 + 2\alpha_2 |A_p|^2 + 3\alpha_3 |A_p|^4$ account for linear and nonlinear loss. We then construct the total electric fields at each (z, t) by use of an effective index, n_{eff} , to account for the linear phase accumulation associated with $\omega_{(p,i,s)}$. We neglect the underlying material dispersion because the dispersion time for our pulses in AlGaAs structures¹⁰ is 2 orders of magnitude larger than the time scales that we consider in this Letter. The signal energy trapped inside the structure is $E_{\text{trap}} = (S_{\text{eff}}/v_g) \int_{\text{struct}} |A_s|^2 dz$, where S_{eff} is an effective area associated with the cross section of the channel waveguides and microresonators; we assume that $S_{\text{eff}} = 1 \mu\text{m}^2$, which is consistent with typical resonator structures.¹¹

In our simulations we use $n_{\text{eff}} = 3$, $n_2 = 1.1 \times 10^{-4} \text{ cm}^2/\text{GW}$, $\alpha_2 = 0.05 \text{ cm}/\text{GW}$, and $\alpha_3 = 0.08 \text{ cm}^3/\text{GW}^2$, all of which are consistent with typical AlGaAs structures.¹² For linear loss we use $\alpha_1 = 0, 0.7, 2 \text{ dB}/\text{cm}$; both nonzero values are significantly higher than the fundamental bending loss in the microresonators.¹³ At all the coupling points we set $\sigma = 0.98$, which is consistent with experimentally observed values.⁷ The fundamental resonant frequency of a ring is $\omega_{e/o} = c/n_{\text{eff}} R_{e/o}$; therefore, when we choose $R_{e/o}$ via $2\pi R_e = 25 \mu\text{m}$ and $2\pi R_o = 30 \mu\text{m}$, the 60th resonance of the outer rings and the 50th resonance of the enhancement rings both occur at $\lambda = 1.5 \mu\text{m}$.

We simulate Gaussian pump and idler pulses with 20 ps FWHM and with intensities $I_p = 50 \text{ MW}/\text{cm}^2$ and $I_i = 0.5 \text{ MW}/\text{cm}^2$. In Fig. 2 we plot the total signal energy deposited into the structure as a function of time for various values of linear loss. In the absence of both linear and nonlinear loss (solid curve) the signal light builds up to a peak of 165 fJ at $\sim 50 \text{ ps}$, then starts to leave the system until $\sim 140 \text{ ps}$,

past which point a constant amount of energy, 90 fJ, remains in the structure. The generated signal light has a frequency width of $\Delta f = 0.028 \text{ ps}^{-1}$, while the reflection spectrum of the outer resonators (within the 10% reflection points) is 0.011 ps^{-1} . Since only those signal frequencies that experience $\approx 100\%$ reflection by the outer rings are trapped within the structure, the rest of the frequencies leave the structure, which explains the decay in trapped signal energy between 50 and 140 ps. The dotted and dashed-dotted curves in Fig. 2 include the effects of linear loss (0.7 and 2 dB/cm, respectively), 2PA, and 3PA. In these situations the trapped signal energy decays, primarily due to linear loss, with a half-life of 428 ps (150 ps) when $\alpha_1 = 0.7 \text{ dB}/\text{cm}$ (2 dB/cm).

We now turn to the flushing process. We begin by trapping the signal light ($\alpha_1 = 0.7 \text{ dB}/\text{cm}$). In Fig. 3 we plot the signal energy in the structure (dotted curve) and the intensity of the signal light leaving the structure (solid curve). Before 200 ps the signal energy in the structure (dotted curve) evolves exactly like the dotted curve in Fig. 2; however, the

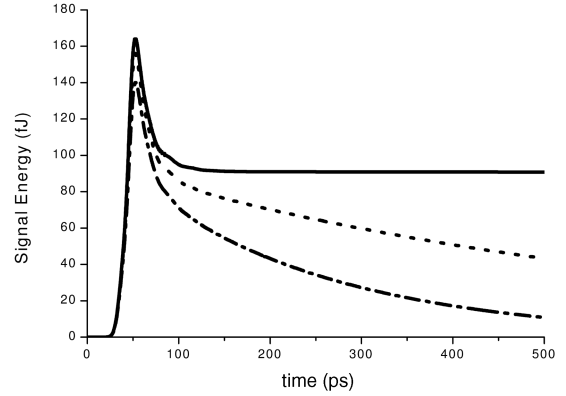


Fig. 2. Energy trapped in the structure as a function of time for linear loss of 0 (solid curve), 0.7 (dotted curve), and 2 dB/cm (dashed-dotted curve).

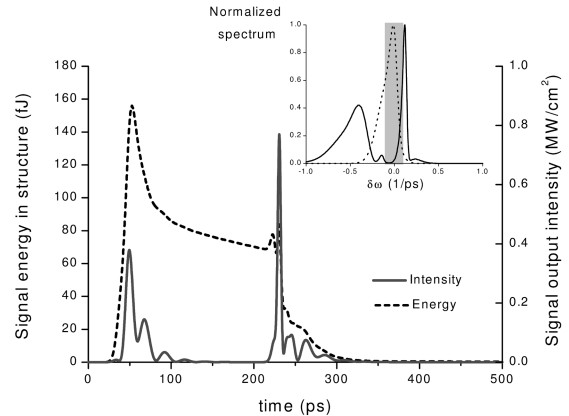


Fig. 3. Energy in the structure (dotted curve) and output signal intensity (solid curve) for the numerical simulation of flushing described in the text. The energy is flushed out at $\sim 200 \text{ ps}$. Inset, frequency spectrum of the flushed signal light as a function of $\delta\omega$, the detuning from the initial signal frequency. The shaded region shows the frequency range over which the outer resonators are 90% reflecting.

solid curve shows that, as discussed above, signal light with frequency content outside the reflection spectrum of the outer resonators leaves the structure between 50 and 140 ps. The 20-ps time lag between peaks in the transient is equal to the round-trip time in the resonator structure. At $t = 200$ ps we inject a Gaussian flush pulse with 20 ps FWHM and peak intensity $I_f = 500$ MW/cm². This causes the trapped signal energy (dotted curve in Fig. 3) to drop sharply from 70 to 30 fJ and then to decay more gradually until almost all the energy has left the system. There is a corresponding jump in the output signal intensity (solid curve) at $t = 220$ ps and then several smaller sidelobes spaced by 20 ps. The small increases in trapped energy at ~ 220 ps are caused by a cascaded process that adds signal energy into the structure by the following process: The flush pulse and the trapped signal light combine to create idler light, which can then interact with the flush pulse to create more signal light. This effect is relatively small and does not affect the ability of the flush pump to remove all the signal light.

The signal light is flushed out of the system because the cross-phase modulation induced by the strong flush pulse leads to an instantaneous frequency shift that detunes the signal light from the outer resonators. To describe this process, we consider the situation in which the signal and flush pulses are propagating along a straight channel waveguide:

$$\left(\frac{\partial}{\partial z} + \frac{1}{v_g} \frac{\partial}{\partial t}\right) A_s(z, t) = i\gamma_s |A_f(z, t)|^2 A_s(z, t). \quad (2)$$

To simplify the discussion, we assume that the intensity envelope function of the flush pulse is only a function of $z - v_g t$, which our numerical calculations indicate is a good qualitative description. We then find that in moving from $z = 0$ to $z = z_o$ the signal pulse accumulates a phase $\phi_{z_o}(t) = i\gamma_s |A_f(z - v_g t)|^2 t$, from which we define the instantaneous frequency: $\omega_{z_o}(t) = -\gamma_s [1 + t(\partial/\partial t)] |A_f(z_o - v_g t)|^2$. To proceed, we assume that the flush pulse intensity profile is Gaussian: $|A_f(z, t)|^2 = I_f \exp[-\beta(z - v_g t)^2]$ so that, from the definition of $\omega_{z_o}(t)$, the signal pulse is blueshifted when $t > (z_o/2v_g) [1 + (1 + 2/\beta z_o^2)^{1/2}]$. In our system the width of the flush pulse is roughly equal to the effective length of the microresonator structure, so that $\beta z_o^2 \approx 1$, and a blueshift occurs for $t \geq \sim 1.35 z_o/v_g$. Note that the center of the flush pulse arrives at z_o when $t = z_o/v_g$, so that in our system both the leading edge and a large part of

the trailing edge of the flush pulse cause a redshift. Therefore the signal light should experience a larger redshift than blueshift. This heuristic description of the flushing dynamics is confirmed by the spectrum of the output signal light (inset in Fig. 3). The shaded region indicates the frequency range within which the outer resonators are $\geq 90\%$ reflecting. It is clear that the frequency of the output signal light has been shifted such that it lies outside the shaded region. Note that the peak frequency of the redshifted light is much further detuned from ω_s than that of the blueshifted light, which is in agreement with the simple picture presented above.

In conclusion we have presented a scheme for trapping light inside a short microresonator structure; the stored light can be extracted with a cross-phase modulation process.

We acknowledge financial support from the Natural Sciences and Engineering Research Council of Canada and Photonics Research Ontario. P. Chak acknowledges the support of an Ontario Graduate Scholarship. His e-mail address is pchak@physics.utoronto.ca.

References

1. P. P. Absil, J. V. Hryniewicz, B. E. Little, P. S. Cho, R. A. Wilson, L. G. Joneckis, and P. T. Ho, *Opt. Lett.* **25**, 554 (2000).
2. J. E. Heebner, R. W. Boyd, and Q.-H. Park, *J. Opt. Soc. Am. B* **19**, 722 (2002).
3. S. Pereira, J. E. Sipe, J. E. Heebner, and R. W. Boyd, *Opt. Lett.* **27**, 536 (2002).
4. S. Pereira, P. Chak, and J. E. Sipe, *J. Opt. Soc. Am. B* **19**, 1991 (2002).
5. S. Pereira, P. Chak, and J. E. Sipe, *Opt. Lett.* **28**, 444 (2003).
6. C. Martijn de Sterke, E. N. Tsoy, and J. E. Sipe, *Opt. Lett.* **27**, 485 (2002).
7. D. Rafizadeh, J. P. Zhang, S. C. Hagness, A. Taflove, K. A. Stair, S. T. Ho, and R. C. Tiberio, *Opt. Lett.* **22**, 1244 (1997).
8. A. Yariv, *Electron. Lett.* **36**, 321 (2000).
9. D. R. Rowland and J. D. Love, *IEEE Proc. Optoelectron.* **14**, 177 (1993).
10. M. A. Afromowitz, *Solid State Commun.* **15**, 59 (1974).
11. V. Van, T. A. Ibrahim, K. Ritter, P. P. Absil, F. G. Johnson, R. Gover, J. Goldhar, and P. T. Ho, *IEEE Photon. Technol. Lett.* **14**, 74 (2002).
12. A. Villeneuve, C. C. Yang, P. G. J. Wigley, G. I. Stegeman, J. S. Aitchison, and C. N. Ironside, *Appl. Phys. Lett.* **61**, 147 (1992).
13. V. Van, P. P. Absil, J. V. Hryniewicz, and P. T. Ho, *Opt. Lett.* **19**, 1734 (2001).